Article

Chemistry & Biology

A Small Molecule Inhibitor of ATPase Activity of HSP70 Induces Apoptosis and Has Antitumor Activities

Graphical Abstract

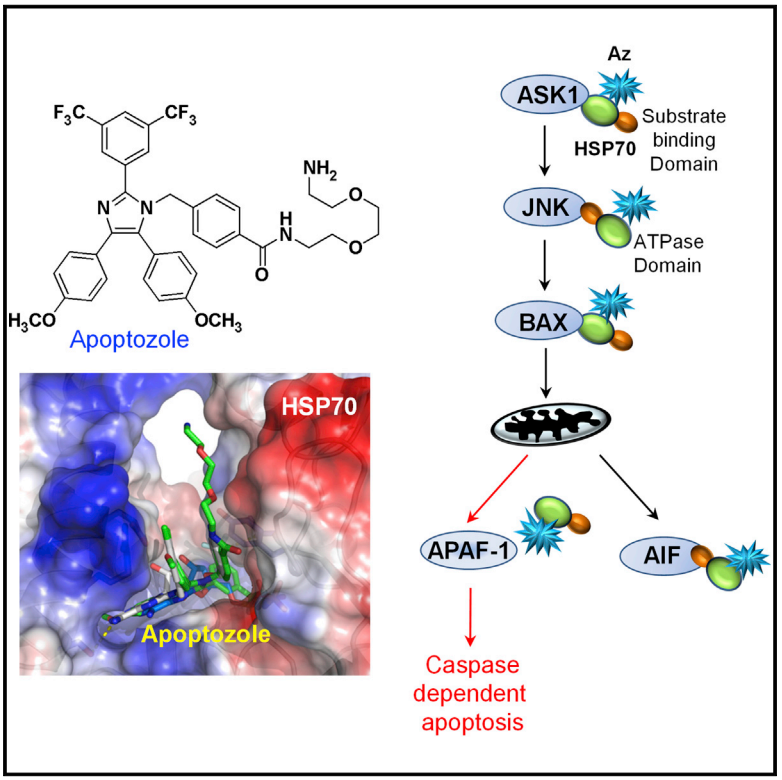

Highlights

- Apoptozole binds HSP70 but not other types of heat shock proteins
- Apoptozole induces caspase-dependent apoptosis
- Apoptozole does not affect interactions of HSP70 with ASK1, JNK, BAX, and AIF
- Apoptozole retards tumor growth in a mouse model without affecting mouse viability

Authors

Sung-Kyun Ko, Jiyeon Kim, ..., Kiwon Song, Injae Shin

Correspondence

injae@yonsei.ac.kr

In Brief

Ko et al. demonstrate that a small molecule, which inhibits an ATPase domain of HSP70, induces caspase-dependent apoptosis by blocking interaction of HSP70 with APAF-1, without affecting interactions of HSP70 with ASK1, JNK, BAX, and AIF. Animal model study shows that the small molecule suppresses tumor growth in mice.

Ko et al., 2015, Chemistry & Biology 22, 391–403
March 19, 2015
http://dx.doi.org/10.1016/j.chembiol.2015.02.004

Chemistry & Biology
Article

A Small Molecule Inhibitor of ATPase Activity of HSP70 Induces Apoptosis and Has Antitumor Activities

Sung-Kyun Ko,[1,6] Jiyeon Kim,[2] Deuk Chae Na,[3] Sookil Park,[1] Seong-Hyun Park,[1] Ji Young Hyun,[1] Kyung-Hwa Baek,[1] Nam Doo Kim,[4] Nak-Kyoon Kim,[5] Young Nyun Park,[3] Kiwon Song,[2] and Injae Shin[1,*]
[1]Center for Biofunctional Molecules, Department of Chemistry, Yonsei University, Seoul 120-749, Korea
[2]Department of Biochemistry, Yonsei University, Seoul 120-749, Korea
[3]Department of Pathology, Yonsei University College of Medicine, Seoul 120-752, Korea
[4]New Drug Development Center, Daegu-Gyeongbuk Medical Innovation Foundation, Daegu 706-010, Korea
[5]Advanced Analysis Center, Korea Institute of Science and Technology, Seoul 136-791, Korea
[6]Present address: Chemical Biology Research Center, Korea Research Institute of Bioscience and Biotechnology (KRIBB), Cheongwon-gun, Chungbuk 363-883, Korea
*Correspondence: injae@yonsei.ac.kr
http://dx.doi.org/10.1016/j.chembiol.2015.02.004

SUMMARY

The heat shock protein HSP70 plays antiapoptotic and oncogenic roles, and thus its inhibition has been recognized as a potential avenue for anticancer therapy. Here we describe the small molecule, apoptozole (Az), which inhibits the ATPase activity of HSP70 by binding to its ATPase domain and, as a result, induces an array of apoptotic phenotypes in cancer cells. Affinity chromatography provides evidence that Az binds HSP70 but not other types of heat shock proteins including HSP40, HSP60, and HSP90. We also demonstrate that Az induces cancer cell death via caspase-dependent apoptosis by disrupting the interaction of HSP70 with APAF-1. Animal studies indicate that Az treatment retards tumor growth in a xenograft mouse model without affecting mouse viability. These studies suggest that Az will aid the development of new cancer therapies and serve as a chemical probe to gain a better understanding of the diverse functions of HSP70.

INTRODUCTION

Apoptosis, or programmed cell death, is a fundamental biological process which is involved in normal development, regulation of the immune system, development of the nervous system, and tissue homeostasis (Baek et al., 2012; Beere, 2005; Newmeyer and Ferguson-Miller, 2003). A large body of literature indicates that the heat shock protein 70 (HSP70) family has multiple functions involved in suppression of apoptotic pathways (Ciocca and Calderwood, 2005; Garrido et al., 2006; Jaattela, 1995; Pocaly et al., 2006; Volloch and Sherman, 1999). The two major cytosolic isoforms of the HSP70 family are HSC70 (a heat shock cognate 70 protein) and HSP70 (an inducible HSC70 homolog protein). Whereas HSC70 is constitutively and ubiquitously expressed, HSP70 is present at relatively low levels in normal cells under non-stressful conditions (Daugaard et al., 2007). However, in response to various stressful stimuli, including heat and oxidative stress, and anticancer agents, the expression level of HSP70 is elevated to protect cells from apoptosis (Lui and Kong, 2007; Mosser et al., 1997; Plumier et al., 1995; Welch and Suhan, 1986). In addition to its role in the stress response, HSP70 displays chaperone activities including protein folding, suppression of the aggregation of denatured proteins, degradation of misfolded proteins, protein translocation, and modulation of the assembly and disassembly of protein complexes (Bukau and Horwich, 1998; Young et al., 2004).

HSP70 consists of an N-terminal ATPase domain (or nucleotide binding domain) and a C-terminal substrate binding domain (SBD) that recognizes polypeptide substrates. The two domains are functionally coupled in such a way that hydrolysis of ATP to ADP by the ATPase activity of HSP70 results in conformational changes in the adjacent SBD that lead to an increase in binding affinities for substrates (Daugaard et al., 2007; Swain et al., 2007). Normally, the ATP-bound form of HSP70 has relatively weak affinity for substrates whereas the ADP-bound protein strongly binds substrates. This feature suggests that ATP hydrolysis is a major driving force for the conformational change and chaperone activity of HSP70.

The expression level of HSP70 is known to increase greatly in various cancers, a phenomenon that leads to tumor cell survival via multiple antiapoptotic processes (Ciocca and Calderwood, 2005; Garrido et al., 2006; Pocaly et al., 2006). Overexpression of HSP70 is correlated with tumor resistance to chemotherapeutic agents, such as imatinib, cisplatin, and etoposide, and poor prognosis in multiple forms of cancer (Gabai et al., 2005; Mosser and Morimoto, 2004; Pocaly et al., 2006). The tumor-protective effects of HSP70 are particularly noticeable when cancer cells are treated with inhibitors (e.g. geldanamycin and its derivatives) of HSP90, a potent target for cancer chemotherapy. Specifically, treatment of cancer cells with these inhibitors results in production of HSP70, thereby leading to a decrease in the cancer cell death effect of HSP90 inhibitors (Bagatell et al., 2000; Wu, 1995).

Owing to its antiapoptotic and oncogenic functions, HSP70 has become an important target for anticancer therapy. To

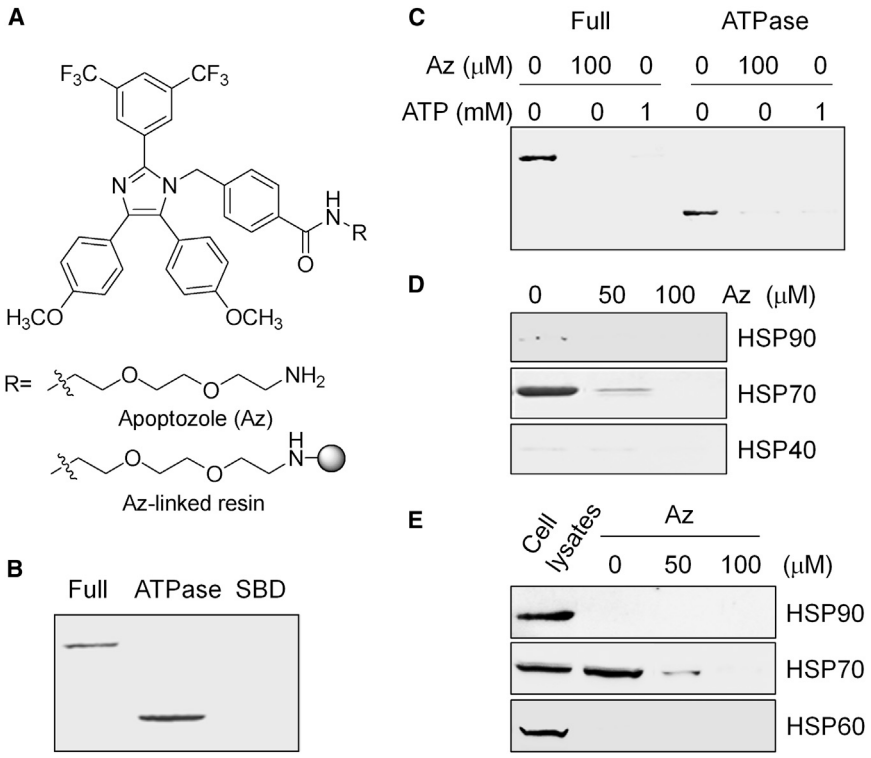

Figure 1. Az Inhibits ATPase Activity of HSP70 by Binding to its ATPase Domain

(A) Chemical structure of Az and Az-linked resin.

(B) Az-linked resin was incubated with purified full-length or truncated HSP70. Proteins bound to the resin were visualized using silver staining.

(C) ATP-agarose resin was incubated with purified full-length and the ATPase domain of HSP70 in the absence or presence of 100 μM Az or 1 mM ATP. Proteins bound to the resin were visualized using silver staining.

(D) Az-linked resin was incubated with purified HSP90, HSP70, and HSP40 in the absence and presence of Az. Proteins bound to the resin were visualized using silver staining.

(E) Az-linked resin was incubated with HeLa cell lysates treated with Az for 1 hr. Bound proteins were analyzed by western blot.

date, several small molecules that bind to HSP70 proteins have been developed for use as potential therapeutic agents and/or chemical probes (Evans et al., 2010; Powers and Workman, 2007). For example, 15-deoxyspergualin (15-DSG), which binds to the C-terminal EEVD domain of HSC70 and HSP90 but not to HSP70, has immunosuppression and low anticancer activities (Kaufman et al., 1996; Nadler et al., 1992). However, 15-DSG has poor bioavailability and its mode of action has not been well elucidated. Dihydropyrimidine derivatives have also been identified as an inhibitor of the ATPase activity of HSP70 (Fewell et al., 2004). Although these substances have modest anticancer activities (Koren et al., 2010), further studies are needed to understand the molecular mechanism of their biological effects. Phenylethynesulfonamide (PES), which binds to the C terminus of HSP70 but not to HSC70 and HSP90, has been shown to kill cancer cells, presumably by disrupting the autophagic process but not by inducing apoptosis (Leu et al., 2009). Rhodacyanine MKT-077 has been observed to have antiproliferative activity against cancer cells by binding in close proximity to the ATP binding site of HSP70 (Wadhwa et al., 2000). However, the use of this molecule as a therapeutic agent is limited because of its rapid metabolism. Although some progress in developing small molecules that bind to HSP70 has been made, an intense effort is required to discover more efficacious inhibitors of HSP70 for cancer therapy and to better understand the diverse functions of HSP70, including its antiapoptotic role.

We recently identified the novel apoptosis-inducing small molecule, apoptozole (Az, Figure 1A), which binds to both HSP70 and HSC70 with similar affinities (Williams et al., 2008b; Cho et al., 2015). However, the detailed apoptotic effect of Az on cancer cells and mechanisms underlying Az-induced apoptosis have not been elucidated. In the effort described below, we have uncovered evidence supporting the conclusion that Az inhibits HSP70 activity by binding to its ATPase domain, and treatment of cancer cells with this substance induces an array of apoptotic phenotypes. The results of cell-based mechanistic studies show that Az blocks the interaction of HSP70 with APAF-1 (apoptotic peptidase activating factor 1) without interfering with its binding to ASK1 (apoptosis signal-regulating kinase 1), JNK (c-Jun N-terminal kinase), BAX, and AIF (apoptosis-inducing factor). Consequently, this substance induces cell death via caspase-dependent apoptosis. In addition, we have shown that Az greatly retards tumor growth in mice xenografted with cancer cells without affecting mouse viability. The combined results arising from cell experiments and animal studies suggest that Az has the potential of being used as an antitumor agent.

RESULTS

Az Blocks ATPase Activity of HSP70 by Binding to the ATPase Domain

The results of previous affinity chromatography studies suggest that HSP70 (an inducible form) and HSC70 (a constitutive form) are primary targets of Az (Williams et al., 2008b). As inducible HSP70 is highly expressed in cancer cells to suppress apoptosis, the current study focusing on HSP70 was carried out to elucidate the molecular mechanism of apoptosis induced by Az. In the initial phase of this effort, we determined which domain of HSP70 was associated with Az. For this purpose, full-length and truncated (ATPase domain and SBD) HSP70 proteins were purified in the N-terminal His_6-tagged forms (Figure S1A). The results of affinity chromatography studies using an Az-linked resin show that the full-length protein and the ATPase domain bind to the resin, but SBD does not (Figure 1B). To further demonstrate that Az binds selectively to the ATPase domain of HSP70, ATP-agarose was incubated with the full-length protein and the ATPase domain in the absence and

presence of 100 μM Az or 1 mM ATP as a competitor. Whereas both proteins bind to the ATP-resin in the absence of Az and ATP, addition of each of these substances leads to a marked decrease in binding of the proteins to ATP-agarose (Figure 1C). Next, the ability of Az to inhibit the ATPase activity of HSP70 was evaluated. The results of a malachite green assay (Cho et al., 2011), which is used to determine monophosphate released from ATP, show that Az inhibits the ATPase activity of HSP70 by 32% at 100 μM and 65% at 200 μM in the presence of 200 μM ATP (Figure S1B).

To examine whether Az binds to other types of heat shock proteins, purified HSP90, HSP70, and HSP40 (Figure S1A) were individually incubated with an Az-linked resin in the absence and presence of Az (50 or 100 μM). As the results in Figure 1D show, while HSP70 binds to the Az-linked resin, HSP90 and HSP40 do not. In addition, we incubated the Az-linked resin with HeLa cell lysates in the absence and presence of Az (50 or 100 μM). The results of affinity chromatography show that HSP60 and HSP90 do not bind to the Az-linked resin (Figure 1E). Taken together, the observations indicate that Az inhibits the ATPase activity of HSP70 by binding to its ATPase domain and that it does not bind to other types of heat shock proteins.

Binding Mode of Az to HSP70

To gain an understanding of the binding mode of Az to HSP70, nuclear magnetic resonance (NMR) and molecular modeling studies were performed. Saturation transfer difference (STD) NMR is a popular ligand-based NMR method used to probe ligand-protein interactions at atomic resolution (Meyer and Peters, 2003; Viegas et al., 2011). In particular, this NMR technique provides ligand-specific binding information. A sample containing 10 μM ATPase domain of HSP70 and 1 mM Az in 20 mM of deuterated Tris buffer (pD 7.0) was found to display a reproducible and well-resolved spectrum. The results of STD NMR data analysis show that all the benzene ring protons of Az (H7, H8, H10, H11, H13, H14, H16, and H17) display large STDs (Figures S2A and S2B), suggesting that they are positioned in close proximity to the binding site of the protein. However, the H1–H6 and H9 protons show only a small level of saturation, suggesting that they only slightly contribute to binding to the protein. These results provide evidence to support the proposal that Az binds to the ATPase domain of HSP70 presumably through interactions of its aromatic rings with residues in the protein binding site.

Two-dimensional (2D) ^{1}H-^{1}H NOESY NMR experiments were conducted to gain information about the conformation of unbound Az. The NMR data yielded a range of conformations of this substance (Figures S2C and S2D), which were then subjected to computational analysis to elucidate the low energy conformation of free Az (Figure S2E). The conformational information and STD NMR data were utilized for molecular docking studies with HSP70 (PDB code 4IO8, a VER-155008 complex form; and PDB code 2E8A, an AMP-PNP [adenylyl-imidodiphosphate, a non-hydrolyzable analog of ATP] bound form) to obtain a more detailed view of the binding mode of Az to HSP70 (Cho et al., 2011; Schlecht et al., 2013; Shida et al., 2010). The results of a molecular modeling study show that Az adopts a conformation that is closely overlaid with AMP-PNP in the ATP binding site of HSP70 (Figure 2A). Specifically, the 3,5-bis(trifluoromethyl) phenyl group of Az interacts with residues in the site that bind to the phosphate moiety of AMP-PNP through polar interactions (Muller et al., 2007), and the 4-methoxyphenyl moiety at the R_2 position of Az is positioned in the adenine binding site of the protein where it interacts with the side chain of Ser275 via hydrogen bonding. On the other hand, the 4-methoxyphenyl group at R_3 in Az interacts with the side chain of Arg272 via the cation-π interaction and a benzyl group in Az via the π-π interaction. The combined results suggest that Az binds to the ATP binding site of HSP70 in a manner similar to that previously observed for its binding to HSC70, which has a high sequence and structural homology with HSP70 (Cho et al., 2011).

In an effort to understand the structural features responsible for inhibition of the ATPase activity of HSP70 by Az, 15 members (**1**–**15**) of a focused imidazole library were prepared using solid support and solution-based methods (Figure 2B) (Kim et al., 2014; Williams et al., 2007, 2008a, 2008b). Effects of the Az analogs on inhibition of the ATPase activity of HSP70 were evaluated using a malachite green assay (Figure 2C). The results show that **1** and **4**, which contain two electron withdrawing groups (CF_3 or CO_2Me) on a phenyl group at R_1, display higher inhibitory activities than analogs with electron donating (**5**–**7**) or single electron withdrawing groups (**2, 3**). This finding suggests that the R_1 moiety of Az is likely located at the binding site of a phosphate moiety of ATP in HSP70 for polar interactions (vide supra).

Imidazole derivatives **8** and **9**, in which 4-methoxy groups present at R_2 and R_3 positions in Az are replaced by electron withdrawing groups (Cl or Br), display lower inhibitory activities than Az or **10**, which possesses electron donating 4-methyl groups. This phenomenon could be explained by the reduced cation-π interaction between an R_3 moiety and the side chain of Arg272. However, a derivative **11** with 4-dimethylaminophenyl groups at these positions exhibits a lower inhibitory activity than Az, a possible result of steric hindrance between R_2 and the binding site of the protein. This proposal is supported by the observation that **12**–**14** containing large fused aromatic rings at R_2 have low inhibitory activities. When the $NH(CH_2)_2O(CH_2)_2NH_2$ moiety in Az is replaced by NH_2 (see **15**), the inhibitory activity is slightly attenuated, suggesting that $NH(CH_2)_2O(CH_2)_2NH_2$ is involved in the interaction of Az with the protein to a certain extent, as shown in STD NMR data. Overall, Az displays the highest ATPase inhibitory activity among the tested compounds. Furthermore, this structure-activity relationship study suggests that although the size and position of substituents attached to phenyl rings in Az affect binding to HSP70, incorporation of electron withdrawing groups at R_1 and electron donating groups at R_2 and R_3 are required to sustain inhibitory activity toward HSP70.

Az Induces Apoptosis in Cancer Cells

Previous studies have served to show that HSP70 acts as an anti-apoptotic protein to promote cancer cell survival (Powers and Workman, 2007). To investigate the effect of Az on cancer cell viability, several cancer cell lines (A549, lung adenocarcinoma epithelial cells; HeLa, cervical cancer cells; MDA-MB-231, breast cancer cells; HepG2, liver cancer cells) were treated with various concentrations (0–15 μM) of Az or compound **7** as a negative control for 18 hr. Cell viabilities were then determined using

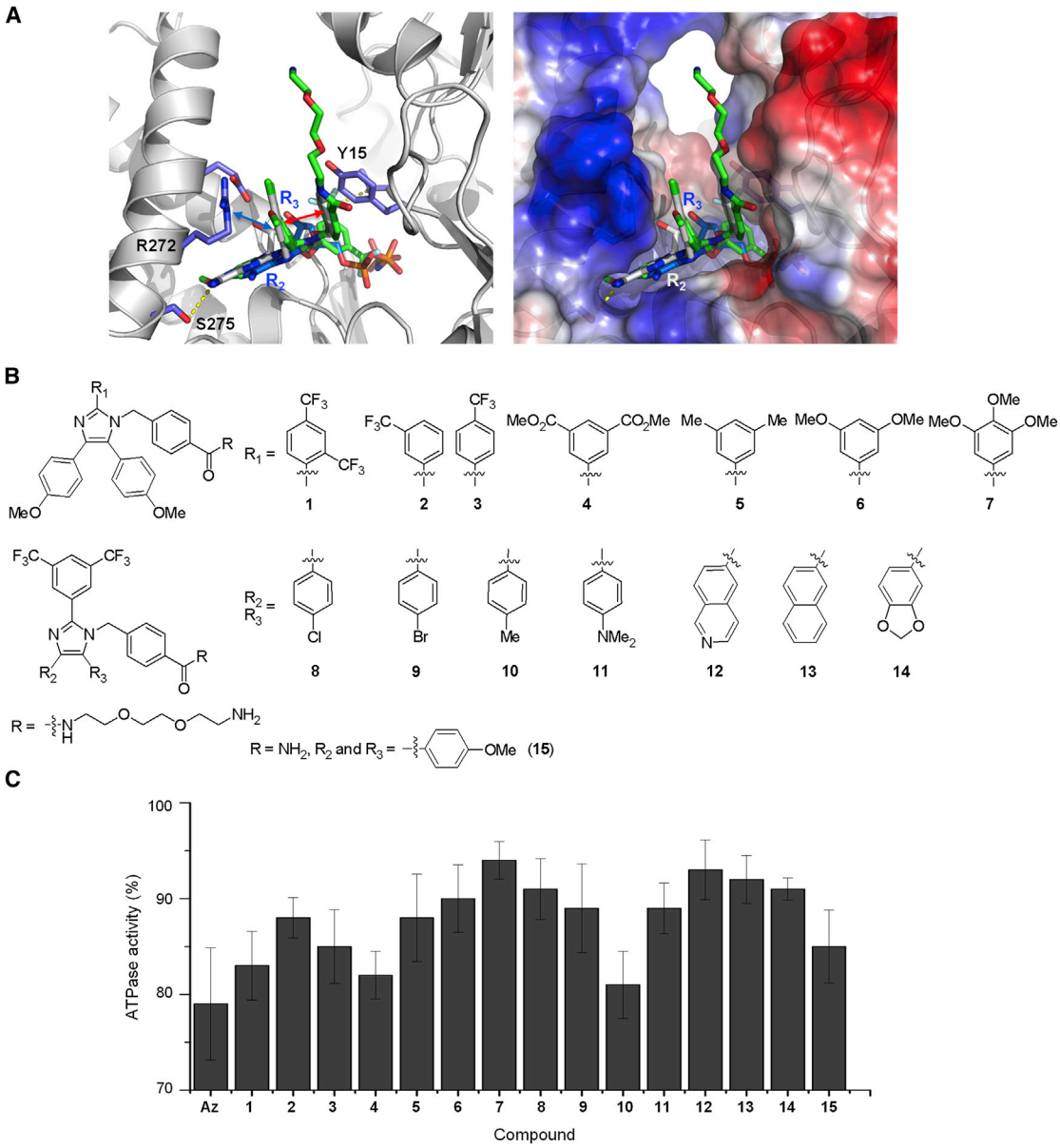

Figure 2. Structure-Activity Relationships

(A) (Left) Docking model of Az (green)/HSP70 superimposed on AMP-PNP (blue, adenosine; orange, β,γ-imidotriphosphate). Red and cyan arrows denote intramolecular π-π stacking and intermolecular cation-π interactions, respectively. (Right) An electrostatic potential surface of the Az binding site of HSP70. Red shows regions of negative charge and blue denotes regions of positive charge.

(B) Structure of Az derivatives **1**–**15**.

(C) Inhibition of ATPase activity of an ATPase domain of HSP70 by the analogs. ATPase activities were measured using a malachite assay after incubation of an ATPase domain with 100 μM of each compound and 50 μM ATP (mean ± SD).

an MTT (3-(4,5-dimethylthiazol-2-yl)-2,5-diphenyltetrazolium bromide) assay. The number of viable cells was found to decrease in an Az dose-dependent way with half maximal inhibitory concentration (IC_{50}) values that ranged from 5 to 7 μM, unlike compound **7** which did not show cytotoxicity (Figures S3A and S3D). In addition, when the incubation times of Az were extended to 48 and 72 hr before conducting the MTT assay, the IC_{50} values were observed to decrease to the nanomolar range (0.9–1.0 μM for 48 hr and 0.7–0.8 μM for 72 hr) (Figures S3B and S3C).

The MTT assay is a widely used method for the measurement of cell death, although it does not discriminate between apoptosis and necrosis. To elucidate whether Az induces cancer cell death via apoptosis, A549 cells were incubated with 8 μM Az for 18 hr and then treated with a mixture of fluorescein-annexin V and propidium iodide (PI). The results of flow cytometry analysis show that Az induces apoptosis, as inferred from the observation of positive annexin V binding and PI uptake, characteristic features of late apoptosis (Figure 3A) (Ko

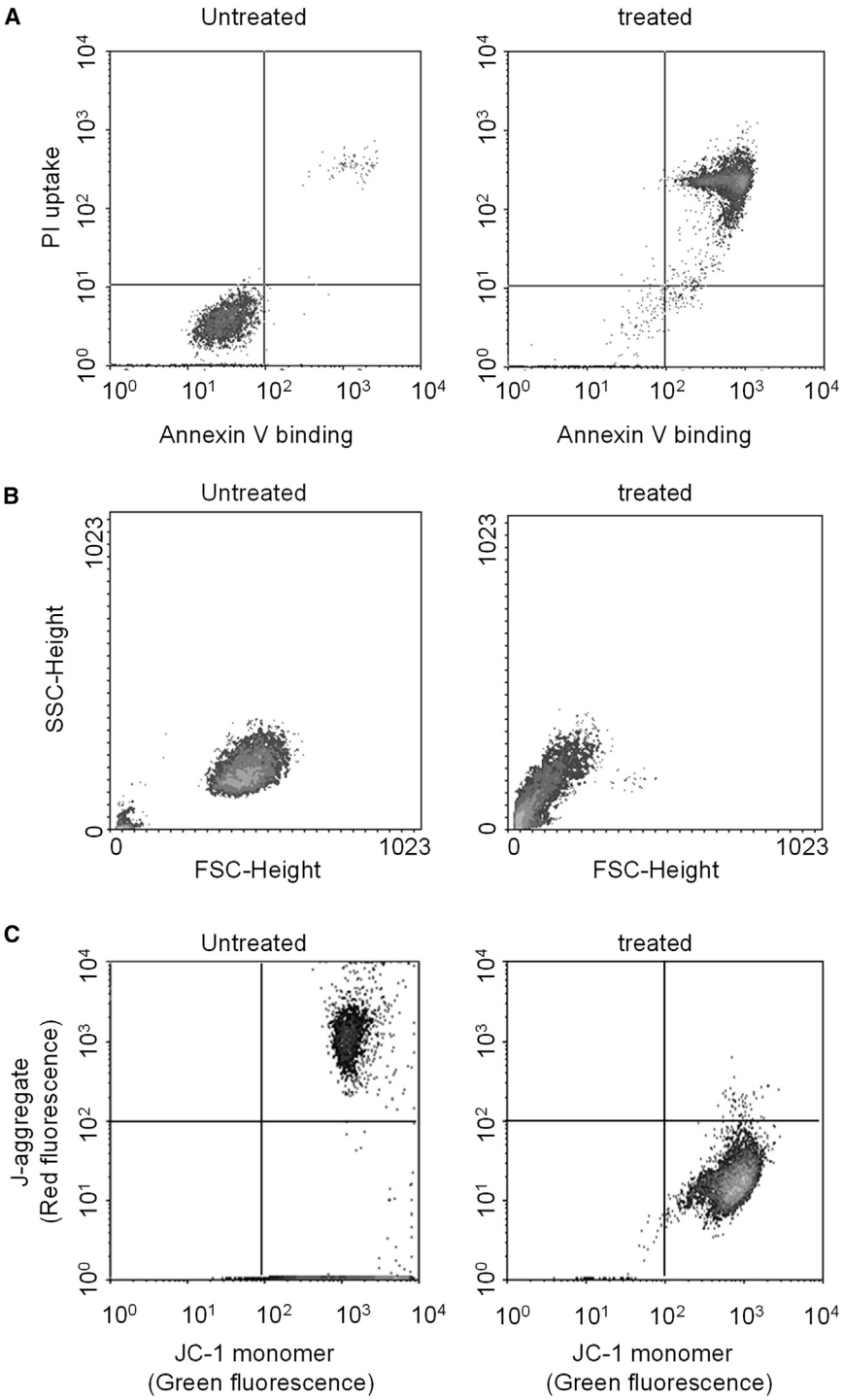

Figure 3. Az Induces Apoptosis

Untreated cells are shown as a negative control.

(A) Flow cytometry of A549 cells treated with 8 μM Az for 18 hr and then stained with a mixture of FITC-annexin V and PI (annexin V versus PI uptake).

(B) A549 cells were treated with 8 μM Az for 18 hr. Cell size was determined using flow cytometry.

(C) Flow cytometry of A549 cells treated with 8 μM Az for 18 hr and then stained with JC-1. A dot plot of green fluorescence (FL1, JC-1 monomer) versus red fluorescence (FL2, JC-1 aggregate) is shown.

et al., 2014). Analysis of cell size by flow cytometry revealed that Az-treated cells exhibit a large degree of cell shrinkage (Figure 3B). Because cell death via necrosis induces cell swelling, this observation serves as additional evidence to support the proposal that the treated cells undergo apoptosis. The loss of mitochondrial membrane potential, a hallmark of apoptosis, was also examined using a JC-1 probe that is sensitive to membrane potential (Smiley et al., 1991). The intensity of dye derived red fluorescence in cells treated with 8 μM Az for 18 hr was found to decrease markedly, as is expected for apoptotic cell death (Figure 3C). Moreover, other typical apoptotic phenotypes, such as loss of cell adherence, condensed cytoplasm, and apoptotic bodies, are also observed microscopically in the Az-treated cells. The combined results provide clear evidence that Az has apoptosis-inducing activity.

Az Does Not Disrupt Associations of HSP70 with ASK1, JNK, and BAX

An investigation was conducted to gain additional information about the cellular mechanism by which inhibition of the ATPase activity of HSP70 by Az promotes apoptosis. ASK1 is known to be activated under various stress conditions to induce apoptotic cell death (Park et al., 2001; Tobiume et al., 2001). HSP70 suppresses apoptosis by inhibiting ASK1 activation through the physical interaction of its ATPase domain with ASK1 in an ATP-independent manner (Figure S4A) (Park et al., 2002). It has been also reported that HSP70 suppresses apoptosis by inhibiting both JNK activation and JNK-mediated apoptosis through direct binding of its SBD to JNK, independent of the chaperone activity of HSP70 (Smiley et al., 1991; Yaglom et al., 1999). In addition, it is known that the translocation of the proapoptotic protein BAX to the mitochondria induces apoptotic cell death (Gotoh et al., 2004). Although not yet thoroughly studied, this process is suppressed by direct binding of HSP70 to BAX in which the ATPase domain of HSP70 is necessary.

Based on these observations, the question of whether or not Az interferes with interactions of HSP70 with ASK1, JNK, and BAX during Az-induced apoptosis was explored. For this purpose, HeLa cells were treated with 5 or 10 μM Az for 18 hr,

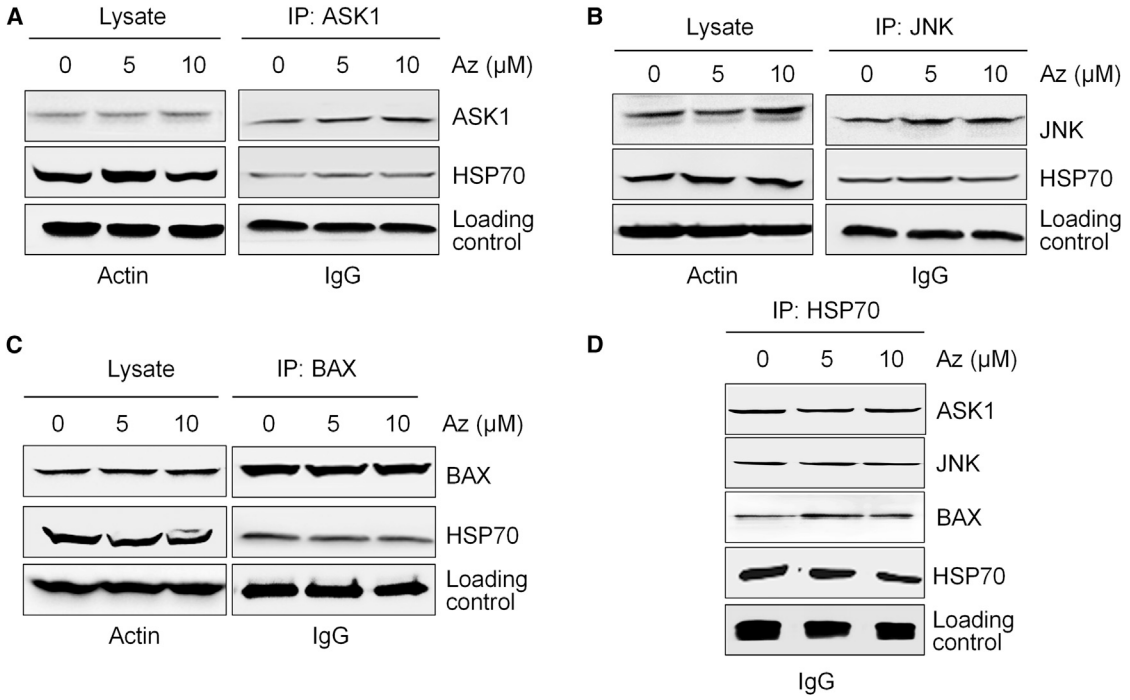

Figure 4. Az Does Not Affect Binding of HSP70 to ASK1, JNK, and BAX

HeLa cells were treated with Az for 18 hr. Immunoprecipitation was performed with (A) ASK1, (B) JNK (C) BAX, and (D) HSP70 antibodies, and the amount of HSP70, ASK1, JNK, and BAX co-precipitated with each protein was determined by western blot.

after which ASK1 and JNK were immunoprecipitated using the corresponding antibodies. Endogenous HSP70 in co-immunoprecipitated complexes of HSP70 with ASK1 or JNK was detected by western blot analysis. The results show that Az neither blocks the association of HSP70 with ASK1 and JNK nor does it affect the expression levels of HSP70, ASK1, and JNK (Figures 4A, 4B, and 4D). The effects of Az on the activation of ASK1 and JNK were also examined by evaluating the levels of their phosphorylated forms in treated cells. The results of immunoblot analysis show that Az treatment does not lead to production of phosphorylated ASK1 and JNK (Figure S5A).

Next, to evaluate the effect of Az on the association of HSP70 with BAX, we determined the amount of BAX co-immunoprecipitated with HSP70 that was produced after HeLa cells were treated with 5 or 10 μM Az for 18 hr. The results show that the expression level of BAX and the amount of HSP70 interacting with BAX remain unchanged in the treated cells (Figures 4C and 4D). Because it is not known which domain of HSP70 interacts with BAX, we investigated this by incubating HeLa cell lysates with purified full-length or truncated (ATPase domain and SBD) HSP70. Immunoblot analysis shows that BAX binds to both full-length and the ATPase domain of HSP70 irrespective of the presence of Az, but does not interact with the SBD (Figure S5B). The results indicate that BAX binds to the ATPase domain of HSP70 but that ATPase activity of HSP70 is not required for this binding. Taken together, the results show that Az does not block interactions of HSP70 with ASK1, JNK, and BAX, and that the ATPase activity of HSP70 is not essential for these interactions.

Az Does Not Induce AIF-Mediated Caspase-Independent Apoptosis

HSP70 has been known to directly interact with AIF to suppress its translocation to the nucleus, thus leading to blockage of caspase-independent apoptosis (Figure S4) (Beere et al., 2000; Ravagnan et al., 2001; Susin et al., 1999). Because of this phenomenon, we determined whether Az blocks the association of HSP70 with AIF to induce cell death via caspase-independent apoptosis. HeLa cells were treated with 5 or 10 μM Az for 18 hr, after which AIF or HSP70 was immunoprecipitated. The results of probing these precipitates using each antibody show that the amount of HSP70 bound to AIF is not changed by treatment of the cells with Az (Figure 5A). In addition, observations made in immunocytochemical analysis indicate that treatment with Az does not induce AIF translocation to the nucleus (Figure 5B). Because Az inhibits the ATPase activity of HSP70, which is not required for the interaction with AIF (Ravagnan et al., 2001), this substance does not influence HSP70 binding to AIF and, consequently, it does not induce cell death via AIF-mediated, caspase-independent apoptosis.

Az Blocks Association of HSP70 with APAF-1

Several studies have served to demonstrate that HSP70 halts progression of the caspase-dependent apoptotic pathway by direct binding of SBD of HSP70 to APAF-1 (Beere et al., 2000; Saleh et al., 2000). To examine whether Az induces caspase-dependent apoptosis by blocking the association of HSP70 with APAF-1, HeLa cells were treated with 5 or 10 μM Az or compound **7** as a negative control for 18 hr, after which cell lysates were immunoisolated using HSP70 and APAF-1 antibodies.

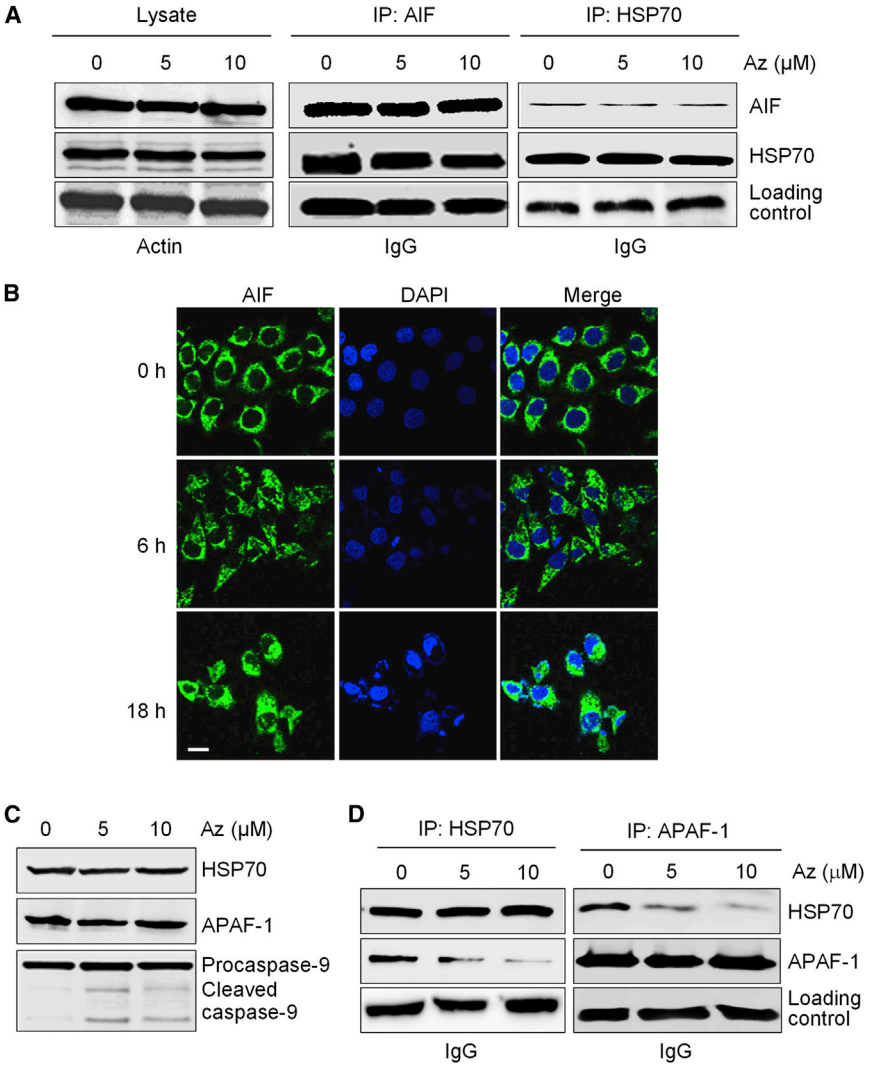

Figure 5. Az Does Not Interfere with Interaction of HSP70 with AIF but Blocks HSP70 Binding to APAF-1

(A) HeLa cells were treated with Az for 18 hr, and immunoprecipitation performed with AIF or HSP70 antibody. The amount of co-precipitated HSP70 or AIF was determined by western blot.

(B) HeLa cells were treated with 6 μM Az for 6 and 18 hr, and processed for immunofluorescence microscopy. Cells were immunostained with AIF antibody and nuclei were visualized with DAPI. Scale bar, 20 μm.

(C) HeLa cells were treated with Az for 18 hr, and indicated proteins were immunoblotted with the corresponding antibodies.

(D) HeLa cells were treated with Az for 18 hr, and immunoprecipitation performed with HSP70 or APAF-1 antibody. The amount of co-precipitated APAF-1 or HSP70 was determined by western blot.

The results of immunoblot analysis demonstrate that treatment with increasing amounts of Az leads to a gradual decrease in the amount of APAF-1 associated with HSP70 without affecting the expression level of APAF-1 (Figures 5C and 5D). However, compound **7** did not affect the association of HSP70 with APAF-1 (Figure S5C). If caspase-dependent apoptosis takes place in Az-treated cells, APAF-1 should activate procaspase-9 to generate a proteolytically cleaved caspase-9 (Beere et al., 2000; Saleh et al., 2000). The results of western blot analysis show that cleaved procaspase-9 is produced in the treated cells (Figure 5C).

To exclude the possibility that Az has off-target effects, HeLa cells were transfected with an HSP70 overexpression vector or an empty vector as a control and then treated with 5 or 10 μM Az for 18 hr. Compared with the control transfected with empty vector, HSP70-transfected cells were found to contain significantly elevated levels of HSP70 (Figure S5D). The results of immunoprecipitation analysis show that the amount of APAF-1 bound to HSP70 is nearly unchanged in HSP70-transfected cells treated with Az (Figure S5D), indicating that HSP70 is the cellular target of Az. Since the ATPase activity of HSP70 is essential for association with APAF-1(Ravagnan et al., 2001), Az prevents this interaction and induces caspase-dependent apoptosis.

Az Induces Caspase Activation

To gain further support for the proposition that Az induces cell death via caspase-dependent apoptosis, the effect of this substance on caspase activation was investigated by measuring proteolytic activities associated with caspases. The activities of caspases in lysates of HeLa cells treated with various concentrations (0–10 μM) of Az for 18 hr were measured using the colorimetric assay with the peptide substrate, Ac-DEVD-pNA (pNA, *p*-nitroaniline). Increases in caspase activity were observed to take place in an Az concentration-dependent manner (Figure S5E). However, when Ac-DEAD-CHO, a known inhibitor of caspases, was added to the lysates of cells treated with Az, caspase activities were greatly attenuated.

As APAF-1 activation and subsequent caspase-9 activation lead to the cleavage of procaspase-3 to produce active caspase-3 (Li et al., 1997), we examined caspase-3 activation by incubating A549 and HeLa cells with 5 or 10 μM Az for 18 hr. Immunoblot analysis reveals that procaspase-3 is proteolytically cleaved to generate caspase-3 (Figure S5F). The results of additional experiments aimed at detecting cleavage of the endogenous caspase substrate, PARP, by western blot analysis show that the cleavage product of PARP is produced in Az-treated cells. However, activation of caspase-3 and cleavage of PARP do not take place to appreciable extents in HSP70-transfected cells treated with Az (Figure S5G), indicating that this small molecule induces caspase activation by inhibiting HSP70 activity.

Next, we evaluated whether the pan-caspase inhibitor ZVAD-FMK (benzyloxycarbonyl-Val-Ala-Asp(OMe) fluoromethylketone), which is a cell-permeable, irreversible caspase inhibitor with broad specificity (Nicholson et al., 1995), protected cells

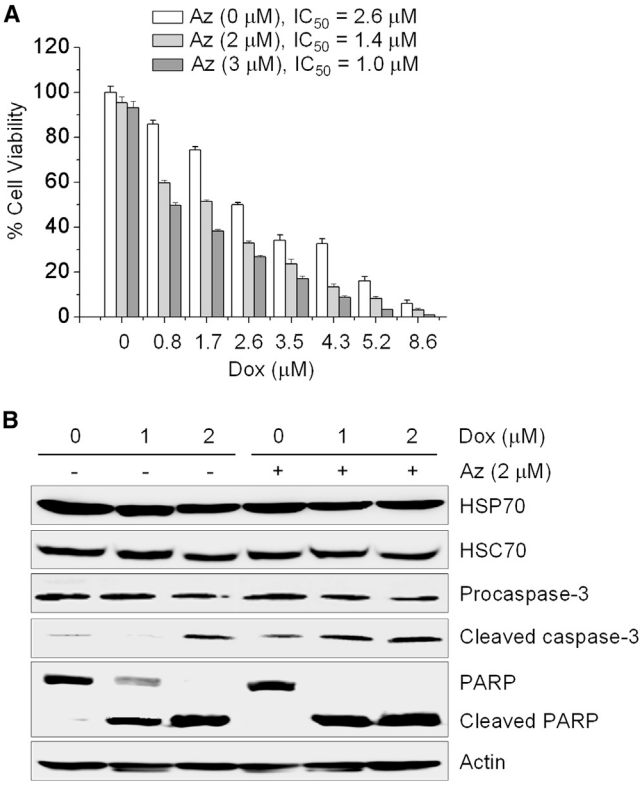

Figure 6. Combined Effect of Az with Dox on Cell Death

(A) A549 cells were treated with Dox alone or a combination of Dox and Az for 12 hr. Cell viabilities were measured using the MTT assay (mean ± SD).

(B) A549 cells were treated with Dox in the presence and absence of 2 μM Az for 12 hr. Activated caspase-3 expression, PARP cleavage, and HSC70 and HSP70 expression levels were determined by western blot.

against the effect of Az. For this purpose HeLa cells, pre-treated with 20 or 40 μM ZVAD-FMK for 3 hr, were incubated with various concentrations (0–8 μM) of Az for 18 hr. Under these conditions the cells were greatly protected from apoptotic cell death induced by Az (Figure S5H). The results of western blot analysis provide further evidence that caspase activation induced by Az is blocked by treatment with 20 μM of the inhibitor (Figure S5I). Taken together, these observations demonstrate that Az-induced cell death occurs via caspase-dependent apoptosis.

Combined Treatment of Az and Doxorubicin Enhances Apoptosis of Cancer Cells

It has been reported that HSP70 renders cells resistant to chemotherapy, and that the overexpression of HSP70 protects cancer cells from antitumor agents such as doxorubicin (Dox) (Demidenko et al., 2006). Thus, it is possible that treatment of cancer cells with a combination of a HSP70 inhibitor and Dox would enhance cancer cell death in comparison with treatment with only one of these substances. To test this proposal, A549 and HeLa cells were co-incubated with Az (0–3 μM) and Dox (0–8.6 μM) for 12 hr. Cell viabilities were then determined using an MTT assay. The results show that the effect of the combined treatment on cell death is more profound than that promoted by Dox alone (Figures 6A and S6A). In both A549 and HeLa cells, IC_{50} values of Dox in the presence of 3 μM Az are approximately half those of Dox alone (2.6 μM of IC_{50} of Dox at 0 μM Az versus 1.0 μM of IC_{50} at 3 μM Az for A549 cells; 3.5 μM of IC_{50} of Dox at 0 μM Az versus 1.7 μM of IC_{50} at 3 μM Az for HeLa cells). Immunoblot analysis revealed that caspase-3 activation and PARP cleavage occur in cells treated with a combination of Az and Dox (Figures 6B and S6B). These findings show that inhibition of HSP70 by Az may be especially powerful in combination with other chemotherapeutic agents for cancer treatment.

Az Inhibits Tumor Growth in Mouse Models

We next turned our attention to an assessment of the therapeutic potential of Az in vivo. For this purpose, the pharmacokinetic properties of Az were examined using a mouse model, administering the substance (10 mg/kg) by an intraperitoneal route. The values of the parameters were compared with those obtained after intraperitoneal injection of Dox into rat (Reddy and Murthy, 2004). The elimination half-life time ($T_{1/2}$) of Az in blood was found to be significantly longer than that of Dox (8.04 versus 1.60 hr) and the time needed to reach a maximum concentration (T_{max}) of Az was shorter than that of Dox (1.00 versus 4.00 hr) (Figure S7A; Table S1). These findings indicate that Az appears more rapidly and is present for a longer time in blood than is Dox after injection.

The efficacy of Az in the nude mice xenografted with A549, RKO (colorectal carcinoma), and HeLa cells was assessed next. Az was injected intraperitoneally at 4 mg/kg every other day for 2 weeks. The sizes of the A549, RKO, and HeLa xenografts, measured over a 30-day period, were found to be smaller in mice treated with Az than in mice treated with the vehicle (Figure 7A). Specifically, compared with the vehicle-treated group, 61%, 65%, and 68% volume reductions of the respective A549, RKO, and HeLa xenografts took place in Az-treated mice.

The antitumor effect of a combination of Az and Dox was also examined in the nude mice xenografted with HeLa cells. The results reveal that treatment with both Az and Dox is more effective in reducing tumor volume in mice than treatment with either agent alone. Specifically, 68%, 61%, and 81% reductions in tumor volumes occur in mice treated with Az and Dox independently, and a combination of Az and Dox, respectively, compared with those of a vehicle-treated group (Figure 7A). Importantly, no significant loss of body weight takes place in mice treated with Az or a combination of Az and Dox (Figures S7B–S7D). In addition, diarrhea- and treatment-related death was not observed in the Az-treated group.

To evaluate Az-induced apoptosis of cancer cells in mice, terminal deoxynucleotidyl transferase-mediated deoxyuridine triphosphate nick end-labeling (TUNEL) values were determined as the ratio of TUNEL-positive cells to total cell numbers in tumor xenografts (Gavrieli et al., 1992). In the absence of Az treatment, the number of TUNEL-positive cells was found to be less than 7% (Figure 7B). However, Az treatment causes a significant increase in TUNEL-positive cells in mice. The number of apoptotic cells in Az-treated mice is more than 40% in the mice bearing the A549, RKO, and HeLa cells. Importantly, combined treatment with Az and Dox leads to apoptosis in 81% of the tumor cells, whereas Az or Dox alone induces apoptosis in 41% and 26% of the tumor cells, respectively. The observations made in the animal model studies provide evidence that Az effectively kills

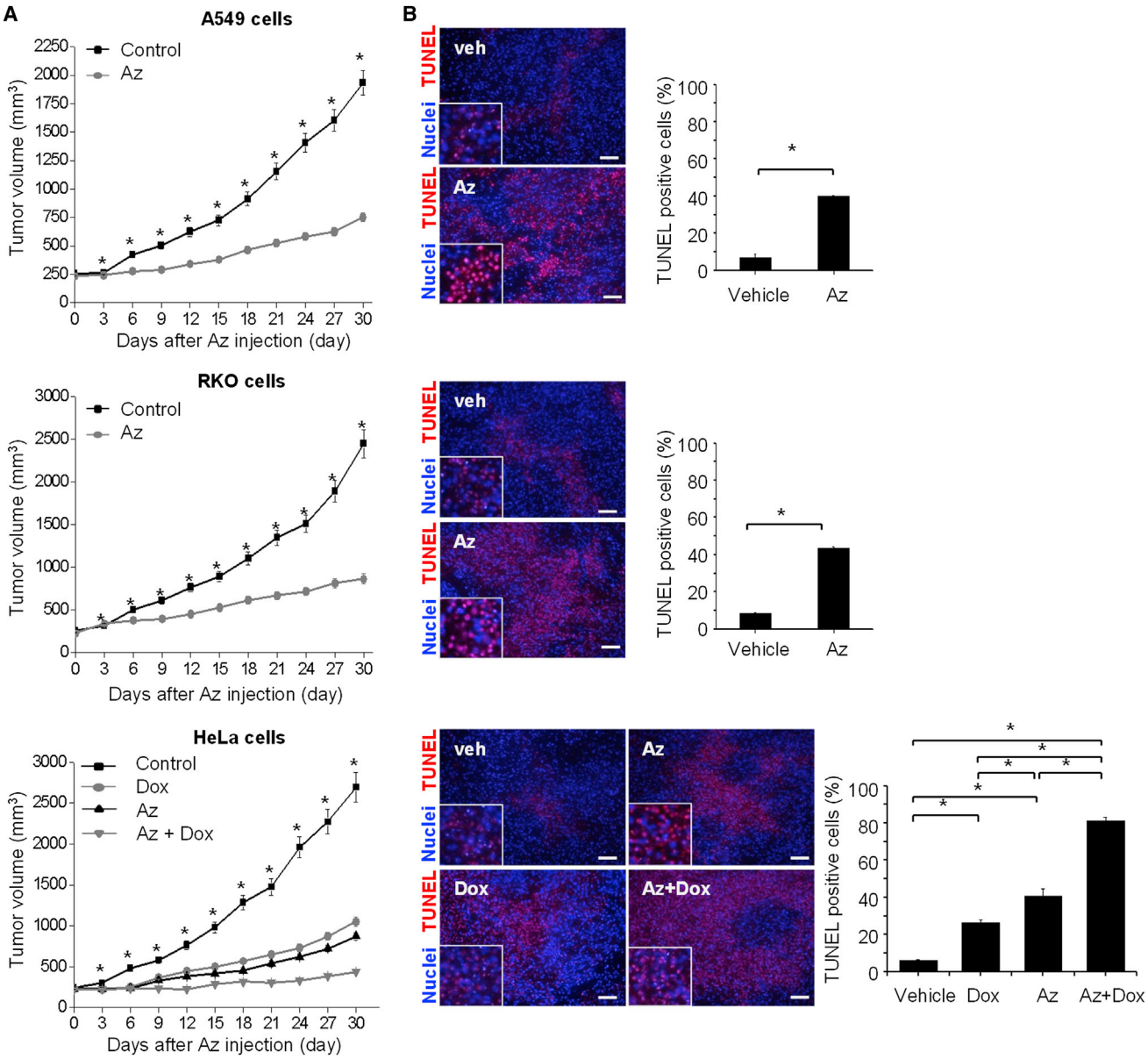

Figure 7. Effect of Az on a Tumor-Xenografted Mouse Model

(A) Effect of Az treatment on the growth of tumor xenografts in nude mice (n = 10). Az was injected intraperitoneally into mice at 4 mg/kg/day every other day for 2 weeks and tumor volumes were determined every 3 days over a 30-day period after Az injection.

(B) A TUNEL assay was performed to evaluate Az-induced apoptosis of tumor xenografts in mice. (Left) Fluorescence images of vehicle, Az-, Dox-, and Az + Dox-treated tumors in mice (red, TUNEL; blue, DAPI). Scale bar, 10 μm. (Right) The bar graphs show the percentage of TUNEL-positive nuclei relative to the total number of nuclei in each section (mean ± SD, $^*P < 0.01$).

cancer cells in mice via the apoptotic process and that the effect of Az is enhanced when it is used in combination with Dox.

DISCUSSION

It is known that the expression level of HSP70 is markedly increased in various cancers, and this upregulation leads to the survival of cancer cells via multiple antiapoptotic processes. High levels of HSP70 are associated with tumor development, resistance to chemotherapy, and poor prognosis in cancer. As a consequence, HSP70 has become a highly attractive target for cancer chemotherapy. This study demonstrates that Az binds to HSP70 but not to other heat shock proteins such as HSP40, HSP60, and HSP90, suggesting that Az is able to overcome the selectivity limitation of HSP70 inhibitors. The results of STD NMR and molecular docking studies suggest that Az binds to an ATP binding site of HSP70 and, as a result, inhibits ATPase activity of the protein. The findings of mechanistic studies in cells reveal that Az blocks binding of HSP70 to APAF-1 without affecting its binding to ASK1, JNK, BAX, and AIF, indicating

that Az induces cancer cell death via caspase-dependent apoptosis (Figure S4). Our results demonstrate that inhibition of ATPase activity of HSP70 is enough to sensitize cancer cells to apoptosis. In mouse studies, we have also observed that administration of Az leads to a marked retardation of tumor growth and an increase in the number of apoptotic cells. More interesting is the finding that combined treatment with Az and Dox induces a greater antiapoptotic activity in cancer cells and antitumor activity in tumor xenografts than that promoted by treatment with either agent alone. This result indicates that Az could play a unique role in anticancer therapy through its use in combination with existing chemotherapeutics to reduce required doses and, consequently, toxic side effects. It has been reported that simultaneous reduction of the expression of both HSP70 and HSC70 with siRNA induces apoptosis of cancer cells but does not result in induction of apoptosis in non-tumorigenic cells (Powers et al., 2008). Because Az suppresses ATPase activities of both HSP70 and HSC70, it has good antitumor activity without side effects, as shown in our animal model study. It is expected that Az could aid the development of new cancer chemotherapies and serve as a chemical probe in studies aimed at gaining a better understanding of the diverse functions of HSP70.

SIGNIFICANCE

The chaperone protein HSP70 acts as an antiapoptotic factor to protect cells from various apoptotic stresses. This protein is upregulated in many cancer types and its overexpression is associated with tumor development, increased resistance to chemotherapy, and poor prognosis. Therefore, small molecule inhibitors of HSP70 have received great attention as potent anticancer agents. We have investigated whether our small molecule, Az, which inhibits the ATPase activity of HSP70 by binding to its ATPase domain, is sufficient for inducing cancer cell death via apoptosis. Initial affinity chromatography study shows that Az binds HSP70 but not other types of heat shock proteins, indicating that Az has selective inhibitory activity toward HSP70. We have demonstrated that an inhibitor of ATPase activity of HSP70 indeed induces an array of apoptotic phenotypes in cancer cells. We have also examined whether this substance induces cancer cell death via caspase-dependent or -independent apoptosis, or both. Our results show that Az induces caspase-dependent apoptosis by blocking the interaction of HSP70 with APAF-1, while not affecting the interaction of HSP70 with ASK1, JNK, BAX, and AIF. Animal model study exhibits that Az suppresses tumor growth in a xenograft mouse model. More significantly, the antitumor activity of Az is greatly enhanced in combination with Dox in cells and mouse. The present investigation could aid the development of novel cancer chemotherapies.

EXPERIMENTAL PROCEDURES

Synthesis of Apoptozole Derivatives

Compounds **1–15** were prepared according to a known procedure (Cho et al., 2015).

NMR Study

NMR spectra were recorded on an Agilent DD2 600-MHz NMR spectrometer equipped with a TR probe at 298 K. The one-dimensional STD NMR data were collected using a 2-s transfer delay and 1,024 scans. On-resonance irradiation of a mixture of Az and protein was set at −1.0 ppm, and off-resonance irradiation at 31.6 ppm. The protons in the spectrum of Az were unambiguously assigned using 2D COSY and 2D NOESY NMR data and inter-proton distances were determined from normalized cross-peak volumes in the 2D NOESY NMR spectrum. A sample containing 1 mM Az (a phosphate salt, formed by mixing 1 equivalent Az and 2 equivalent phosphoric acid) and 10 μM ATPase domain of HSP70 was prepared in deuterated Tris buffer (pD 7.0) for NMR measurements.

Molecular Modeling

The crystal structure of HSP70 from the PDB (code 4IO8, a VER-155008 bound form) was used for docking simulations. The structure of Az was built using the Maestro build panel and minimized using the Impact module of Maestro in the Schrödinger suite program. The starting coordinates of HSP70 were further modified for Glide docking. The HSP70/VER-155008 complex was imported to Maestro and the ligand was removed from the structure. Water molecules were removed and hydrogen atoms were added to the crystal structure of HSP70. The protein structure was minimized using the Protein Preparation Wizard by applying an OPLS (optimized potentials for liquid simulations) force field. For grid generation, the binding site was defined as the centroid of the VER-155008. Ligand docking into the ATP binding site of HSP70 was carried out using the Schrödinger docking program, Glide. Energy minimized Az was docked into the prepared receptor grid. The best-docked pose was selected as the lowest Glide score. Molecular graphics for the inhibitor binding pocket and refined docking model for the selected Az were generated using the PyMol package (http://www.pymol.org).

Cell Culture

The A549 (lung cancer cells), HeLa (cervical cancer cells), MDA-MB-231 (breast cancer cells), and HepG2 (liver cancer cells) cells were obtained from the American Type Culture Collection and grown in RPMI 1640 (Invitrogen) supplemented with 10% fetal bovine serum (FBS), 50 units/ml penicillin, and 50 units/ml streptomycin. Cells were maintained at 37°C under a humidified atmosphere of 5% CO_2.

Affinity Chromatography Using Az-Linked and ATP Resins

Az-linked resin or ATP-agarose (Sigma-Aldrich) in bead buffer (10 mM Tris [pH 7.4], 5 mM NaF, 250 mM NaCl, 5 mM EDTA, 5 mM EGTA, 0.1% Triton X-100, and one tablet of protease inhibitor cocktail [Roche] per 20 ml buffer) was incubated with 2–5 μg of purified proteins (full-length and truncated HSP70, HSP40, and HSP90) at 4°C for 1 hr. In competition experiments, 100 μM Az or 1 mM ATP was added to each protein in bead buffer, and the mixture was incubated at 4°C for 30 min. Az-linked resin or ATP-agarose was incubated with the protein pre-treated with the competitor and washed several times with 1 ml of bead buffer. Proteins bound to the resin were collected with 30 μl of Laemmli buffer (Bio-Rad) at 94°C for 5 min and separated using 10% SDS-PAGE for silver staining and western blot analysis.

Measurements of ATPase Activities of HSP70

A master mix of an ATPase domain of HSP70 (final concentration 2 μM) was prepared in assay buffer (100 mM Tris-HCl, 20 mM KCl, and 6 mM $MgCl_2$ [pH 7.4]). An aliquot (10 μl) of this mixture and 9 μl of Az in assay buffer were added to a 96-well plate and incubated for 30 min at room temperature. The reaction was started by adding 1 μl of 4 mM ATP. After 3 hr of incubation at 37°C, 80 μl of malachite green reagent was added to each well and was incubated at 37°C for 15 min, and 10 μl of 34% sodium citrate was added to halt the non-enzymatic hydrolysis of ATP. The absorbance was determined at 620 nm with a SpectraMax 340 PC 384 (Molecular Devices). To correct for non-enzymatic hydrolysis of ATP, the absorbance of a sample formed from an identically treated ATP buffer lacking the protein was subtracted.

MTT Assay

Cells (5×10^3 per well) were plated in triplicate in 96-well plates in 0.1 ml of culture media with 10% FBS. After 24 hr, cells were treated with various concentrations of Az (0–15 μM) in culture media with 3% FBS (final volume: 0.2 ml per well) for 18, 48, and 72 hr before treatment with MTT. MTT assays were performed according to general procedures. Absorbance at 570 nm was

measured using a UV microplate reader (SpectraMax 340PC 384; Molecular Devices).

Western Blot Analysis

Proteins were separated by 6%–12% SDS-PAGE. Mouse HSP60 monoclonal (1:1000, Santa Cruz Biotechnology), mouse HSP70 monoclonal (1:1000, StressGen Biotechnology), mouse HSP90 monoclonal (1:1000, Santa Cruz Biotechnology), rabbit caspase-9 polyclonal (1:1000, Santa Cruz Biotechnology), mouse procaspase-3 monoclonal (1:1000, Santa Cruz Biotechnology), rabbit cleaved caspase-3 polyclonal (1:1000, Santa Cruz Biotechnology), rabbit PARP polyclonal (1:1000, Cell Signaling Technology), rabbit AIF polyclonal (1:1000, Santa Cruz Biotechnology), rabbit BAX polyclonal (1:1000, Santa Cruz Biotechnology), rabbit JNK polyclonal (1:1000, Santa Cruz Biotechnology), rabbit ASK1 polyclonal (1:1000, Santa Cruz Biotechnology), and mouse APAF-1 monoclonal (1:1000, Santa Cruz Biotechnology) antibodies were used as primary antibodies. Horse peroxidase-conjugated goat anti-mouse immunoglobulin G (IgG) (1:5000, Sigma-Aldrich) was used as the secondary antibody, and the treated membranes were visualized using the ECL kit (Amersham Biosciences). Quantitative data were obtained with ImageQuant version 5.2 (Molecular Dynamics) and Origin version 8.0 (Microcal).

Immunocytochemistry

HeLa cells pre-incubated with Az were fixed with 4% formaldehyde in PBS buffer for 15 min and processed for immunostaining. The cells were incubated with rabbit AIF polyclonal antibody (1:200, Santa Cruz Biotechnology) for 1 hr at room temperature followed by incubation with Alexa-Fluor 488 conjugated rabbit IgG (1:200, Invitrogen/Molecular Probes) for 0.5–1 hr at room temperature and mounted with DAPI (Invitrogen/Molecular Probes). The cells were imaged by confocal fluorescence microscopy (Zeiss).

Flow Cytometry

A549 cells were treated with 8 μM Az for 18 hr. Untreated cells were used as a negative control. After washing with PBS twice, the cells were incubated with 0.5 ml of trypsin-EDTA (0.05% trypsin, 0.02% EDTA; Sigma-Aldrich) for 5–10 min at 37°C and collected. Cells were re-suspended in binding buffer (500 μl, 10 mM HEPES/NaOH [pH 7.5] containing 1.4 M NaCl and 2.5 mM $CaCl_2$) and treated with a mixture of fluorescein-annexin V (final concentration 0.5 μg/ml) and PI (final concentration 2 μg/ml) for 10 min at room temperature. For JC-1 staining, cells were re-suspended with PBS containing JC-1 (final concentration 2.5 μg/ml; Anaspec), incubated for 15 min, and washed with PBS twice. Flow cytometry was performed using FACSCalibur (BD Biosciences) and CellQuest software (Becton Dickinson). The red fluorescence signal was measured using excitation wavelength of 550 nm and emission wavelength of 600 nm, and the green fluorescence using 485-nm excitation and 535-nm emission.

Caspase Activity Assay

Caspase activity was determined using acetyl-DEVD-pNA (Sigma-Aldrich), a preferred substrate for caspase-3 and -7. The enzyme-catalyzed release of pNA was monitored at 405 nm using a UV microplate reader.

Immunoprecipitation

HeLa cells were treated with 5–10 μM Az for 18 hr in parallel with an untreated negative control. Cells were lysed with 1× RIPA buffer (50 mM Tris-HCl [pH 8], 150 mM NaCl, 1% NP-40, 0.5% sodium deoxycholate, and one tablet of protease inhibitor cocktail) for 10 min at 4°C and centrifuged at 10,000 rpm for 10 min. Cell lysates were pre-cleared with 20 μl of the appropriate suspended (25%, v/v) agarose conjugate (protein A-agarose or protein G-agarose, Invitrogen) for 30 min at 4°C and incubated with primary antibodies for 2 hr at 4°C. To capture antibody on the resin, antibody-treated lysates were incubated with protein A-agarose or protein G-agarose on the rotator at 4°C overnight. Immunoprecipitates were collected and analyzed by western blots.

Antitumor Activity in Mouse

Male nude mice were purchased from Orient Bio Co. The animals were housed in a pathogen-free room under controlled temperature and humidity. The animal study was conducted according to the established procedures of the Yonsei University Laboratory Animal Maintenance Manual. Mice aged 4 weeks were injected with tumor cells for the xenograft experiments. Viable A549 and RKO cells (5×10^6) and HeLa cells (5×10^6) were injected subcutaneously into the flank of mice. The A549 and RKO cell xenograft mice were immediately and randomly assigned to two groups. The first group (n = 10) was used as a control group and received vehicle only. The second group (n = 10) received intraperitoneal injections of Az (4 mg/kg/day) every other day for 2 weeks. The HeLa cell xenograft mice were immediately and randomly assigned to four groups. The first group (n = 10) was a control group receiving vehicle only. The second group (n = 10) received intraperitoneal injections of Az (4 mg/kg/day) every other day for 2 weeks. The third group (n = 10) received intraperitoneal injections of doxorubicin (15 mg/kg/day) every other day for 2 weeks. The fourth group (n = 10) received intraperitoneal injections of Az (4 mg/kg/day) and doxorubicin (15 mg/kg/day) every other day for 2 weeks. Tumors in all mice were measured in two dimensions with calipers every 3 days and tumor volumes were calculated using the formula volume = $w \times l^2/2$, where w is the width at the widest point of the tumor and l is the length perpendicular to w. The results from individual mice were plotted as average tumor volumes versus time.

Combined Treatment of Apoptozole and Doxorubicin

A549 and HeLa cells were plated in triplicate in 0.1 ml in 96-well plates for 24 hr and treated with various concentrations of doxorubicin alone or a combination of doxorubicin (0.8–8.6 μM) with Az (2 or 3 μM). After 12 hr, cells were analyzed by the MTT assay and western blots as described above.

Statistical Analysis

All data are reported as means ± SD. Statistical significance of differences between control and experimental groups was determined using two-groups two-tailed Student's t test, with a level of statistical significance of $P < 0.01$.

SUPPLEMENTAL INFORMATION

Supplemental Information includes Supplemental Experimental Procedures, seven figures, and one table and can be found with this article online at http://dx.doi.org/10.1016/j.chembiol.2015.02.004.

AUTHOR CONTRIBUTIONS

I.S., Y.N.P., and K.S. designed the study and supervised the work. S.-K.K., J.K., D.C.N., S.-H.P., and K.-H.B. performed cell and animal studies. S.P. synthesized compounds. J.Y.H. and N.-K.K. carried out the NMR study. N.-D.K. performed the molecular modeling study.

ACKNOWLEDGMENTS

This work was supported by grants from the National Creative Research Initiative (grant no. 2010-0018272 to I.S.) program and the National R&D program for Cancer Control (grant no. NCCR-0920300). A part of this work was carried out with support from the Korea government (MSIP) (grant no. NRF-2013R1A2A2A05005990 to Y.N.P.).

Received: November 12, 2014
Revised: January 20, 2015
Accepted: February 5, 2015
Published: March 12, 2015

REFERENCES

Baek, K.-H., Park, J., and Shin, I. (2012). Autophagy-regulating small molecules and their therapeutic applications. Chem. Soc. Rev. *41*, 3245–3263.

Bagatell, R., Paine-Murrieta, G.D., Taylor, C.W., Pulcini, E.J., Akinaga, S., Benjamin, I.J., and Whitesell, L. (2000). Induction of a heat shock factor 1-dependent stress response alters the cytotoxic activity of hsp90-binding agents. Clin. Cancer Res. *6*, 3312–3318.

Beere, H.M. (2005). Death versus survival: functional interaction between the apoptotic and stress-inducible heat shock protein pathways. J. Clin. Invest. *115*, 2633–2639.

Beere, H.M., Wolf, B.B., Cain, K., Mosser, D.D., Mahboubi, A., Kuwana, T., Tailor, P., Morimoto, R.I., Cohen, G.M., and Green, D.R. (2000). Heat-shock protein 70 inhibits apoptosis by preventing recruitment of procaspase-9 to the Apaf-1 apoptosome. Nat. Cell Biol. *2*, 469–475.

Bukau, B., and Horwich, A.L. (1998). The Hsp70 and Hsp60 chaperone machines. Cell *92*, 351–366.

Cho, H.J., Gee, H.Y., Baek, K.H., Ko, S.K., Park, J.M., Lee, H., Kim, N.D., Lee, M.G., and Shin, I. (2011). A small molecule that binds to an ATPase domain of Hsc70 promotes membrane trafficking of mutant cystic fibrosis transmembrane conductance regulator. J. Am. Chem. Soc. *133*, 20267–20276.

Cho, H.J., Kim, G.-H., Park, S.-H., Hyun, J.Y., Kim, N.-K., and Shin, I. (2015). Probing of effect of an inhibitor of an ATPase domain of Hsc70 on clathrin-mediated endocytosis. Mol. BioSyst. http://dx.doi.org/10.1039/c4mb00695j.

Ciocca, D.R., and Calderwood, S.K. (2005). Heat shock proteins in cancer: diagnostic, prognostic, predictive, and treatment implications. Cell Stress Chaperones *10*, 86–103.

Daugaard, M., Rohde, M., and Jaattela, M. (2007). The heat shock protein 70 family: highly homologous proteins with overlapping and distinct functions. FEBS Lett. *581*, 3702–3710.

Demidenko, Z.N., Vivo, C., Halicka, H.D., Li, C.J., Bhalla, K., Broude, E.V., and Blagosklonny, M.V. (2006). Pharmacological induction of Hsp70 protects apoptosis-prone cells from doxorubicin: comparison with caspase-inhibitor- and cycle-arrest-mediated cytoprotection. Cell Death Differ. *13*, 1434–1441.

Evans, C.G., Chang, L., and Gestwicki, J.E. (2010). Heat shock protein 70 (hsp70) as an emerging drug target. J. Med. Chem. *53*, 4585–4602.

Fewell, S.W., Smith, C.M., Lyon, M.A., Dumitrescu, T.P., Wipf, P., Day, B.W., and Brodsky, J.L. (2004). Small molecule modulators of endogenous and co-chaperone-stimulated Hsp70 ATPase activity. J. Biol. Chem. *279*, 51131–51140.

Gabai, V.L., Budagova, K.R., and Sherman, M.Y. (2005). Increased expression of the major heat shock protein Hsp72 in human prostate carcinoma cells is dispensable for their viability but confers resistance to a variety of anticancer agents. Oncogene *24*, 3328–3338.

Garrido, C., Brunet, M., Didelot, C., Zermati, Y., Schmitt, E., and Kroemer, G. (2006). Heat shock proteins 27 and 70: anti-apoptotic proteins with tumorigenic properties. Cell Cycle *5*, 2592–2601.

Gavrieli, Y., Sherman, Y., and Ben-Sasson, S.A. (1992). Identification of programmed cell death in situ via specific labeling of nuclear DNA fragmentation. J. Cell Biol. *119*, 493–501.

Gotoh, T., Terada, K., Oyadomari, S., and Mori, M. (2004). hsp70-DnaJ chaperone pair prevents nitric oxide- and CHOP-induced apoptosis by inhibiting translocation of Bax to mitochondria. Cell Death Differ. *11*, 390–402.

Jaattela, M. (1995). Over-expression of hsp70 confers tumorigenicity to mouse fibrosarcoma cells. Int. J. Cancer *60*, 689–693.

Kaufman, D.B., Gores, P.F., Kelley, S., Grasela, D.M., Nadler, S.G., and Ramos, E. (1996). 15-Deoxyspergualin: immunotherapy in solid organ and cellular transplantation. Transplant Rev. *10*, 160–174.

Kim, G.H., Halder, D., Park, J., Namkung, W., and Shin, I. (2014). Imidazole-based small molecules that promote neurogenesis in pluripotent cells. Angew. Chem. Int. Ed. Engl. *53*, 9271–9274.

Ko, S.K., Kim, S.K., Share, A., Lynch, V.M., Park, J., Namkung, W., Van Rossom, W., Busschaert, N., Gale, P.A., Sessler, J.L., et al. (2014). Synthetic ion transporters can induce apoptosis by facilitating chloride anion transport into cells. Nat. Chem. *6*, 885–892.

Koren, J., Jinwal, U.K., Jin, Y., O'Leary, J., Jones, J.R., Johnson, A.G., Blair, L.J., Abisambra, J.F., Chang, L., Miyata, Y., et al. (2010). Facilitating Akt clearance via manipulation of Hsp70 activity and levels. J. Biol. Chem. *285*, 2498–2505.

Leu, J.I., Pimkina, J., Frank, A., Murphy, M.E., and George, D.L. (2009). A small molecule inhibitor of inducible heat shock protein 70. Mol. Cell *36*, 15–27.

Li, P., Nijhawan, D., Budihardjo, I., Srinivasula, S.M., Ahmad, M., Alnemri, E.S., and Wang, X. (1997). Cytochrome c and dATP-dependent formation of Apaf-1/caspase-9 complex initiates an apoptotic protease cascade. Cell *91*, 479–489.

Lui, J.C., and Kong, S.K. (2007). Heat shock protein 70 inhibits the nuclear import of apoptosis-inducing factor to avoid DNA fragmentation in TF-1 cells during erythropoiesis. FEBS Lett. *581*, 109–117.

Meyer, B., and Peters, T. (2003). NMR spectroscopy techniques for screening and identifying ligand binding to protein receptors. Angew. Chem. Int. Ed. Engl. *42*, 864–890.

Mosser, D.D., and Morimoto, R.I. (2004). Molecular chaperones and the stress of oncogenesis. Oncogene *23*, 2907–2918.

Mosser, D.D., Caron, A.W., Bourget, L., Denis-Larose, C., and Massie, B. (1997). Role of the human heat shock protein hsp70 in protection against stress-induced apoptosis. Mol. Cell. Biol. *17*, 5317–5327.

Muller, K., Faeh, C., and Diederich, F. (2007). Fluorine in pharmaceuticals: looking beyond intuition. Science *317*, 1881–1886.

Nadler, S.G., Tepper, M.A., Schacter, B., and Mazzucco, C.E. (1992). Interaction of the immunosuppressant deoxyspergualin with a member of the Hsp70 family of heat shock proteins. Science *258*, 484–486.

Newmeyer, D.D., and Ferguson-Miller, S. (2003). Mitochondria: releasing power for life and unleashing the machineries of death. Cell *112*, 481–490.

Nicholson, D.W., Ali, A., Thornberry, N.A., Vaillancourt, J.P., Ding, C.K., Gallant, M., Gareau, Y., Griffin, P.R., Labelle, M., Lazebnik, Y.A., et al. (1995). Identification and inhibition of the ICE/CED-3 protease necessary for mammalian apoptosis. Nature *376*, 37–43.

Park, H.S., Lee, J.S., Huh, S.H., Seo, J.S., and Choi, E.J. (2001). Hsp72 functions as a natural inhibitory protein of c-Jun N-terminal kinase. EMBO J. *20*, 446–456.

Park, H.S., Cho, S.G., Kim, C.K., Hwang, H.S., Noh, K.T., Kim, M.S., Huh, S.H., Kim, M.J., Ryoo, K., Kim, E.K., et al. (2002). Heat shock protein hsp72 is a negative regulator of apoptosis signal-regulating kinase 1. Mol. Cell. Biol. *22*, 7721–7730.

Plumier, J.C., Ross, B.M., Currie, R.W., Angelidis, C.E., Kazlaris, H., Kollias, G., and Pagoulatos, G.N. (1995). Transgenic mice expressing the human heat shock protein 70 have improved post-ischemic myocardial recovery. J. Clin. Invest. *95*, 1854–1860.

Pocaly, M., Lagarde, V., Etienne, G., Ribeil, J.A., Claverol, S., Bonneu, M., Moreau-Gaudry, F., Guyonnet-Duperat, V., Hermine, O., Melo, J.V., et al. (2006). Overexpression of the heat-shock protein 70 is associated to imatinib resistance in chronic myeloid leukemia. Leukemia *21*, 93–101.

Powers, M.V., and Workman, P. (2007). Inhibitors of the heat shock response: biology and pharmacology. FEBS Lett. *581*, 3758–3769.

Powers, M.V., Clarke, P.A., and Workman, P. (2008). Dual targeting of Hsc70 and Hsp72 inhibits Hsp90 function and induces tumor-specific apoptosis. Cancer Cell *14*, 250–262.

Ravagnan, L., Gurbuxani, S., Susin, S.A., Maisse, C., Daugas, E., Zamzami, N., Mak, T., Jaattela, M., Penninger, J.M., Garrido, C., et al. (2001). Heat-shock protein 70 antagonizes apoptosis-inducing factor. Nat. Cell Biol. *3*, 839–843.

Reddy, L.H., and Murthy, R.S. (2004). Pharmacokinetics and biodistribution studies of doxorubicin loaded poly(butyl cyanoacrylate) nanoparticles synthesized by two different techniques. Biomed. Pap. Med. Fac. Univ. Palacky Olomouc Czech. Repub. *148*, 161–166.

Saleh, A., Srinivasula, S.M., Balkir, L., Robbins, P.D., and Alnemri, E.S. (2000). Negative regulation of the Apaf-1 apoptosome by Hsp70. Nat. Cell Biol. *2*, 476–483.

Schlecht, R., Scholz, S.R., Dahmen, H., Wegener, A., Sirrenberg, C., Musil, D., Bomke, J., Eggenweiler, H.M., Mayer, M.P., and Bukau, B. (2013). Functional analysis of Hsp70 inhibitors. PLoS One *8*, e78443.

Shida, M., Arakawa, A., Ishii, R., Kishishita, S., Takagi, T., Kukimoto-Niino, M., Sugano, S., Tanaka, A., Shirouzu, M., and Yokoyama, S. (2010). Direct inter-subdomain interactions switch between the closed and open forms of the Hsp70 nucleotide-binding domain in the nucleotide-free state. Acta Crystallogr. D Biol. Crystallogr. *66*, 223–232.

Smiley, S.T., Reers, M., Mottola-Hartshorn, C., Lin, M., Chen, A., Smith, T.W., Steele, G.D., Jr., and Chen, L.B. (1991). Intracellular heterogeneity in mitochondrial membrane potentials revealed by a J-aggregate-forming lipophilic cation JC-1. Proc. Natl. Acad. Sci. USA *88*, 3671–3675.

Susin, S.A., Lorenzo, H.K., Zamzami, N., Marzo, I., Snow, B.E., Brothers, G.M., Mangion, J., Jacotot, E., Costantini, P., Loeffler, M., et al. (1999). Molecular characterization of mitochondrial apoptosis-inducing factor. Nature *397*, 441–446.

Swain, J.F., Dinler, G., Sivendran, R., Montgomery, D.L., Stotz, M., and Gierasch, L.M. (2007). Hsp70 chaperone ligands control domain association via an allosteric mechanism mediated by the interdomain linker. Mol. Cell *26*, 27–39.

Tobiume, K., Matsuzawa, A., Takahashi, T., Nishitoh, H., Morita, K., Takeda, K., Minowa, O., Miyazono, K., Noda, T., and Ichijo, H. (2001). ASK1 is required for sustained activations of JNK/p38 MAP kinases and apoptosis. EMBO Rep. *2*, 222–228.

Viegas, A., Manso, J.o., Nobrega, F.L., and Cabrita, E.J. (2011). Saturation-transfer difference (STD) NMR: a simple and fast method for ligand screening and characterization of protein binding. J. Chem. Educ. *88*, 990–994.

Volloch, V.Z., and Sherman, M.Y. (1999). Oncogenic potential of Hsp72. Oncogene *18*, 3648–3651.

Wadhwa, R., Sugihara, T., Yoshida, A., Nomura, H., Reddel, R.R., Simpson, R., Maruta, H., and Kaul, S.C. (2000). Selective toxicity of MKT-077 to cancer cells is mediated by its binding to the hsp70 family protein mot-2 and reactivation of p53 function. Cancer Res. *60*, 6818–6821.

Welch, W.J., and Suhan, J.P. (1986). Cellular and biochemical events in mammalian cells during and after recovery from physiological stress. J. Cell Biol. *103*, 2035–2052.

Williams, D.R., Lee, M.R., Song, Y.A., Ko, S.K., Kim, G.H., and Shin, I. (2007). Synthetic small molecules that induce neurogenesis in skeletal muscle. J. Am. Chem. Soc. *129*, 9258–9259.

Williams, D.R., Kim, G.H., Lee, M.R., and Shin, I. (2008a). Fluorescent high-throughput screening of chemical inducers of neuronal differentiation in skeletal muscle cells. Nat. Protoc. *3*, 835–839.

Williams, D.R., Ko, S.K., Park, S., Lee, M.R., and Shin, I. (2008b). An apoptosis-inducing small molecule that binds to heat shock protein 70. Angew. Chem. Int. Ed. Engl. *47*, 7466–7469.

Wu, C. (1995). Heat shock transcription factors: structure and regulation. Annu. Rev. Cell Dev. Biol. *11*, 441–469.

Yaglom, J.A., Gabai, V.L., Meriin, A.B., Mosser, D.D., and Sherman, M.Y. (1999). The function of HSP72 in suppression of c-Jun N-terminal kinase activation can be dissociated from its role in prevention of protein damage. J. Biol. Chem. *274*, 20223–20228.

Young, J.C., Agashe, V.R., Siegers, K., and Hartl, F.U. (2004). Pathways of chaperone-mediated protein folding in the cytosol. Nat. Rev. Mol. Cell Biol. *5*, 781–791.